Molecular Vision 2023; 29:39-57 <http://www.molvis.org/molvis/v29/39>
Received 13 March 2023 | Accepted 5 May 2023 | Published 14 May 2023

Encephalopsin (OPN3) is required for normal refractive development and the GO/GROW response to induced myopia

Courtney Linne,[1,2,4,5] Khine Yin Mon,[1,2] Shane D'Souza,[1,2,4] Heonuk Jeong,[8,9] Xiaoyan Jiang,[8,9] Dillon M. Brown,[6,7] Kevin Zhang,[1,2,4,5] Shruti Vemaraju,[1,2,3] Kazuo Tsubota,[8,10] Toshihide Kurihara,[8,9] Machelle T. Pardue,[6,7] Richard A. Lang[1,2,3]

[1]Visual Systems Group, Abrahamson Pediatric Eye Institute, Division of Pediatric Ophthalmology, Cincinnati Children's Hospital Medical Center, Cincinnati, OH; [2]Science of Light Center, Cincinnati Children's Hospital Medical Center, Cincinnati, OH; [3]Department of Ophthalmology, College of Medicine, University of Cincinnati, Cincinnati, OH; [4]Molecular & Developmental Biology Graduate Program, University of Cincinnati, College of Medicine, Cincinnati, OH; [5]Medical Scientist Training Program, University of Cincinnati, College of Medicine, Cincinnati, OH; [6]Department of Ophthalmology and Neuroscience Program, Emory University School of Medicine, Atlanta, GA; [7]Center for Visual and Neurocognitive Rehabilitation, Atlanta VA Health Care System, Decatur, GA; [8]Department of Ophthalmology, Keio University School of Medicine, Tokyo, Japan; [9]Laboratory of Photobiology, Keio University School of Medicine, Tokyo, Japan; [10]Tsubota Laboratory, Inc., Tokyo, Japan

Purpose: Myopia, or nearsightedness, is the most common form of refractive error and is increasing in prevalence. While significant efforts have been made to identify genetic variants that predispose individuals to myopia, these variants are believed to account for only a small portion of the myopia prevalence, leading to a feedback theory of emmetropization, which depends on the active perception of environmental visual cues. Consequently, there has been renewed interest in studying myopia in the context of light perception, beginning with the opsin family of G-protein coupled receptors (GPCRs). Refractive phenotypes have been characterized in every opsin signaling pathway studied, leaving only Opsin 3 (OPN3), the most widely expressed and blue-light sensing noncanonical opsin, to be investigated for function in the eye and refraction.

Methods: *Opn3* expression was assessed in various ocular tissues using an Opn3eGFP reporter. Weekly refractive development in *Opn3* retinal and germline mutants from 3 to 9 weeks of age was measured using an infrared photorefractor and spectral domain optical coherence tomography (SD-OCT). Susceptibility to lens-induced myopia was then assessed using skull-mounted goggles with a −30 diopter experimental and a 0 diopter control lens. Mouse eye biometry was similarly tracked from 3 to 6 weeks. A myopia gene expression signature was assessed 24 h after lens induction for germline mutants to further assess myopia-induced changes.

Results: *Opn3* was found to be expressed in a subset of retinal ganglion cells and a limited number of choroidal cells. Based on an assessment of *Opn3* mutants, the OPN3 germline, but not retina conditional *Opn3* knockout, exhibits a refractive myopia phenotype, which manifests in decreased lens thickness, shallower aqueous compartment depth, and shorter axial length, atypical of traditional axial myopias. Despite the short axial length, *Opn3* null eyes demonstrate normal axial elongation in response to myopia induction and mild changes in choroidal thinning and myopic shift, suggesting that susceptibility to lens-induced myopia is largely unchanged. Additionally, the *Opn3* null retinal gene expression signature in response to induced myopia after 24 h is distinct, with opposing *Ctgf*, *Cx43*, and *Egr1* polarity compared to controls.

Conclusions: The data suggest that an OPN3 expression domain outside the retina can control lens shape and thus the refractive performance of the eye. Prior to this study, the role of *Opn3* in the eye had not been investigated. This work adds OPN3 to the list of opsin family GPCRs that are implicated in emmetropization and myopia. Further, the work to exclude retinal OPN3 as the contributing domain in this refractive phenotype is unique and suggests a distinct mechanism when compared to other opsins.

Myopia, or nearsightedness, is a disease in which images are focused in front of the retina due to a mismatch between eye size and refractive power [1]. The cause of myopia is poorly understood but of great importance [2]. Refractive errors, including myopia, are the primary cause of visual impairment worldwide and the second leading cause of blindness [3]. "The Myopia Boom" is the term coined to describe the rapid increase in myopia cases worldwide, predicted to reach 50% of the world's population—5 billion people—by 2050 [4]. Further, although myopic refractive error can be addressed with corrective lenses and laser eye surgery and its

Correspondence to: Richard A. Lang, Division of Pediatric Ophthalmology, Cincinnati Children's Hospital Medical Center, 3333 Burnet Avenue, Cincinnati OH 45229, Phone: 513-636-2700 (Office), 513-803-2230 (Assistant), FAX: 513-636-4317; email: richard.lang@cchmc.org

progression slowed with drug treatment, few new treatments have been proposed in decades [5], and those that do exist are expensive and not very effective [6].

While significant efforts have been made in myopia research to identify potential myopia risk genes [7], these gene variants account for only 18.4% of the variance in refractive error, and many of the identified risk variants are involved in responding to cues from the environment, including phototransduction and circadian rhythms [8]. These results concur with epidemiological studies showing that while myopia varies by nationality, with east Asian countries having the highest prevalence, it also increases dramatically with urbanization (80%–90% in urban east Asian countries) and educational attainment, again supporting environmental causation [9]. Further supporting an environmental etiology, outdoor light exposure has a dose-dependent protective effect on myopia [10-12]. This has led to the development of a theory of emmetropization, or perfect focus, which depends on the active perception of visual cues during development to provide feedback for eye growth [13].

As a result, and especially noting the preventative effect of outdoor light, there has been renewed interest in studying myopia from the perspective of visual perception of light cues, beginning with the opsin family of G-protein coupled receptors (GPCRs). These include the canonical cone (OPN1SW, OPN1MW, OPN1LW) and rod opsins (OPN2) as well as the noncanonical opsins (OPN3, OPN4, and OPN5). The canonical opsins are expressed in conventional photoreceptors and are involved in visual perception, while the noncanonical opsins have widespread light-sensing functions in the retina [14,15], skin [16], adipose tissue [17], and hypothalamus [18].

The investigation of the role of opsins in refractive development has been dependent on recent technological advances, including automated photorefraction [19] and spectral domain optical coherence tomography (SD-OCT). These instruments have made it possible to use the mouse as a myopia model [20]. Mouse myopia has been shown to mirror that of other myopia models, including primates, while providing access to the unique genetic tools of the mouse model [21,22]. Through genetic manipulation made possible by the mouse model, all opsins investigated have been proven to play a role in refractive development, including the expected roles of both rod [23,24] and cone opsins [25,26], and recently, the noncanonical opsins OPN4 [27,28] and OPN5 [29] as well. Only OPN3, a blue-light-sensing noncanonical opsin, remains to be investigated.

OPN3 (also called encephaloopsin or panopsin) is a noncanonical blue-light-sensitive opsin (λ_{max} 470 nm in pufferfish, 500 nm in mosquito [30] and 465 nm in zebrafish [31]). *Opn3* expression was first described in 1999 in the cortex, striatum, cerebellum, and lateral thalamus in mouse [32]. Later, expression was also noted outside the nervous system in the placenta, liver, and kidney [33]. *Opn3* expression can also be detected in the preoptic area of the hypothalamus, the periventricular nucleus, the optic nerve, the iris–ciliary body complex [34], the trigeminal nerve, and in the retina within retinal ganglion cells [35]. In fact, *Opn3* is the most widely expressed mammalian opsin. Despite this wide expression, there has been less research on the functional role of OPN3 compared with other opsins. To date, light sensing has been reported to be OPN3-dependent in white [17] and brown [36] adipose tissue, and this characteristic has been proposed for the trachea [37] and uterus [38]. A light-independent function has been described in skin [39].

Here, we utilize both the germ line and conditional loss-of-function of *Opn3* to assess the role of this opsin in refractive development and induced myopia in mice. These genetic manipulations were combined with an induced myopia model [29]. Our results suggest that an *Opn3* expression domain outside the retina is important for controlling normal lens thickness and depth of the aqueous compartment as well as promoting axial elongation, thus affecting the overall refractive performance of the eye. This finding also suggests that communication between eye tissues may be important for refractive development.

METHODS

Lead contact and materials availability: No new reagents or mouse lines were generated for this study. Further information and resource requests should be directed to the lead contact, Richard A. Lang, Division of Pediatric Ophthalmology, Cincinnati Children's Hospital Medical Center, 3333 Burnet Avenue, Cincinnati OH 45,229, Tel: 513–636–2700 (Office), 513–803–2230 (Assistant), FAX: 513–636–4317. Email: richard.lang@cchmc.org.

Experimental model and subject details:

Mice—All animals were housed in a pathogen-free vivarium according to institutional guidelines. The genetically modified mice used in this study included the following: *Opn3*$^{fl/fl}$ and *Opn3*$^{\Delta Ex2}$ (generated as previously described [17]), *mRx-Cre* [40], and *Tg(Opn3-EGFP)JY3Gsat* (MMRRC stock number 030727-UCD). Opn3^{fl} mice have a mixed *C57Bl6/6N*, *129S4/Sv*, and *B6;FVB* background. All mice were genotyped for a naturally occurring mutation in *Cp49* found in 129 mouse strain that leads to impaired lens translucency in old age [41]. Age-matched male and female

Table 1. Genotyping primers.

Allele	Primers	Pairs	bp
Opn3	F1: ACCCAGGCTTCTTTTGGTCT	F1R1 – Wild-type	1191
	R1: AGAGTCGTTGGCATCCTTGG	F1R1 – Opn3fl	1231
	F2: ACTATCCCGACCGCCTTACT	F1R2 – Opn3fl	1610
	R2: GAACTGATGGCGAGCTCAGA	F1R2 – Opn3cko	640
$Opn3^{\Delta Ex2}$	F1: CTCAGAACCCACAAAGTGCTGG	F1R1 – Wild-type	307
	R1: GTGGACTGCAATGTCCCATCTATC	F1R2 – $Opn3^{\Delta Ex2}$	191
$Opn3^{Tg(Opn3\text{-}EGFP)JY3Gsat}$	F1: CAGAGCGTGAGATCCACCCTGTT	F1R1 – $Opn3^{eGFP}$	320
	R1: TAGCGGCTGAAGCACTGCA		

cohorts of multiple litters, each with their own littermate control, were used for all experiments. Genotyping primers for relevant mouse lines are included in Table 1. All mice were fed standard chow and water ad libitum.

Lighting conditions: Animals were housed in standard fluorescent lighting (photon flux 1.62 × 10^{15} photons cm−2 s−1) on a 12L:12D light/dark cycle until weaning, when they were transferred to full-spectrum lighting. For full-spectrum lighting, LEDs were used to yield a comparable total photon flux of 1.68 × 10^{15} photons/cm^2/sec. The spectral and photon flux information for the LED lighting is as follows: near-violet (λ_{max}=380 nm, 4.23 × 10^{14} photons/cm^2/sec in the 370–400 nm range), blue (λ_{max}=480 nm, 5.36 × 10^{14} photons/cm^2/sec in the 430–530 nm range), and red (λ_{max}=630 nm, 6.72 × 1014 photons/cm^2/sec in the 600–700 nm range). Photon fluxes were measured at approximately 61 cm from the source through an empty standard mouse cage.

Tissue processing: Retinal tissue was processed as previously described [42]. Briefly, mice were anesthetized with isofluorane, followed by cervical dislocation. Then, eyes were enucleated and fixed for 30 min in 4% paraformaldehyde (PFA) in phosphate buffered saline (PBS), rinsed, and stored at 4°C until use. Whole-mount retinae were processed as previously described, using the same method of marking the orientation with a mark at the ventral pole before dissection for topology studies. Sectioned eyes were processed similarly, also as previously described [43].

Staining: Similarly, retinae for immunofluorescence (IHC) were again incubated in 5% PBST and 50% acetone for antigen retrieval and then washed, blocked, and incubated for 3 to 5 days in primary antibody as previously described. Primary antibodies included those against chicken anti-GFP (1:1000, abcam ab290, RRID:AB_303395, Cambridge, UK, abcam.com), rabbit anti-dsRed (1:1000, TakaraBio 632,496, RRID:AB_10013483, Kusatsu, Shiga, Japan, takarabio.com), rabbit anti-Rbpms (1:500, Abcam ab152101), mouse anti-calbindin (1:300, Abcam ab82812, RRID:AB_1658451), rabbit anti-melanopsin (N15, a gift from Ignacio Provencio), and mouse anti-Calretinin (1:300, Sigma Aldrich MAB1568, St. Louis, MO) [43].

RGC overlap assessment: Flat-mount retinal preparations from *Opn5*^{cre}*; Ai14; Opn3-eGFP* mice were imaged using a Nikon A1R confocal microscope. High-resolution large-tiled images corresponding to the superior and inferior regions of the retina were acquired from three animals. Tiles were subdivided into multiple subfields for cell type analysis. Briefly, images were imported into ImageJ (v1.53), and cells were manually characterized into one of seven groups based on the co-expression of tdTomato (reporting the *Opn5*-lineage), GFP (reporting *Opn3* expression), and OPN4 (melanopsin). Cell type assignment was performed using the CellCounter plugin in ImageJ.

Refractive assessment: All mouse lines were tested for normal refractive development and lens-induced myopia (LIM) and measured weekly to quantify refraction and ocular parameter changes. For our LIM model, mouse refraction and ocular parameters were measured at 3 weeks, and then a head pedestal was attached and goggles mounted the next day. Each head pedestal fits one −30D lens over the right eye and a 0D lens over the left eye and was generously provided by Toshihide Kurihara of Keio University [29].

On the day of refractive assessment, five minutes before assessment, the mice had their eyes dilated with 1% tropicamide and were anesthetized with either ketamine (60 mg/kg)/xylazine (7 mg/kg; mixed background) or ketamine (90 mg/kg)/xylazine (10 mg/kg; C57Bl/6J) depending on the strain background. To better preserve the essential tear layer but reduce mouse movement, mice were scruffed, and their refraction was quantified using infrared autorefractometry (Photorefractor, Stria-Tech, Tubingen, Germany). This was performed before full sedation but after the mice lost their equilibrium to prevent disturbing the tear film.

After the mice were fully anesthetized and no longer responsive to a toe pinch, biometric measurements of the mouse eye were taken using a spectral domain optical coherence tomography (SD-OCT) imager (Envisu R-Class, Bioptogen-Leica Microsystems, Wetzlar, Germany, leica-microsystems.com). Eye drops were provided as needed throughout imaging and during recovery, and the mice were kept warm using a heating pad. Ocular parameters included corneal thickness, depth of aqueous, lens thickness, vitreous chamber depth, retinal thickness, axial length, and choroidal thickness. After imaging, the anesthetic was reversed using 5mg/kg atipamezole.

The *Opn3* germline and the *mRx-cre; Opn3*$^{fl/fl}$ lines had slightly different backgrounds due to the method with which they were generated (see "Mice" for more detail). Previous studies have established line-dependent differences in refractive development [44]. This may explain the slight difference in baseline refraction between *Opn3*$^{fl/fl}$ and *Opn3*$^{+/+}$ mice.

Head pedestal surgery: The mice were anesthetized with ventilated isofluorane (induction: 3%, maintenance: 1%–2%), and the top of their heads were shaved. The exposed skin was then cleaned with 3% hydrogen peroxide, and a 1 cm by 1 cm region of skull was exposed. The region was again sterilized with 3% hydrogen peroxide, and the exposed fascia and periosteum were removed. The area was then dried, and dental acrylic (Ortho-Jet, Lang Dental, Wheeling, IL) was used to bond the head pedestal to the mouse to which lenses could be attached. The mice were provided carprofen-medicated diet gel water for three days for analgesia.

GO/GROW RT-qPCR Analysis: The animals were anesthetized with isofluorane followed by cervical dislocation as a secondary form of euthanasia at the same time of day and within a two-hour period to minimize circadian variability. The retina and RPE were then harvested and immediately snap frozen and homogenized in TRI Reagent (Invitrogen, Waltham, MA) using 2.0mm RNase-free zirconium oxide beads in the TissueLyser II sample disrupter (Qiagen, Hilden, Germany). Phase separation was achieved using chloroform, and RNA in the aqueous phase was precipitated using ethanol. The resultant product was then purified using a modified GeneJET RNA purification column (ThermoFisher Scientific #K0732) protocol and eluted into RNase-free water. The RNA was then treated with RNase-free DNase I (ThermoFisher Scientific #EN0521), and cDNA was synthesized using a Verso cDNA synthesis kit (ThermoFisher Scientific AB1453/B). Quantitative RT–PCR was performed with Radiant SYBR Green Lo-ROX qPCR mix (Alkali Scientific Inc.) using a ThermoFisher QuantStudio 6 Flex Real-Time PCR system.

The GO/GROW genes list was adapted from a list developed by He et al. [45], which is a compilation of genes whose expression is changed in a variety of myopia-induction animal models. Validated primers for the relevant GO/GROW signature genes were then obtained from the Harvard PrimerBank [46]. The primer sequences are listed in the Table 2.

Tissue processing, sectioning, and immunofluorescence: The animals were anesthetized with isofluorane and cervically dislocated as a secondary form of euthanasia

Data analysis: All data processing was performed using GraphPad Prism v8 (San Diego, CA). Ocular measurements were quantified using MouseSwimmerV2, a MatLab program generously provided by Machelle Pardue of Georgia Tech/Emory University. Then, a two-way ANOVA with Šidák multiple comparisons was performed to compare *Opn3* mutant animals to controls, with and without goggling, at multiple time points. For the refractive development analysis, the two eyes were averaged, as both eyes received the same treatment. For the goggling experiments, the effect of −30 diopter lenses was calculated by determining the "shift" in the difference in measurement between the −30 diopter (right) and the 0 diopter (left) eye. To eliminate inter-subject variability, all ocular and refractive measurements were normalized to their initial baseline values before calculating the shift.

For the RT-qPCR experiments, the relative expression of GO/GROW signature genes was calculated using the $^{\Delta\Delta}$Ct method by first normalizing to a control gene (Tbp) run on the same plate and then determining the relative expression of the target gene versus the geometric mean of the control eyes. Next, paired *t* tests were used to assess differences between goggled and non-goggled eyes. All data are expressed as an average ± standard error of the mean, with the significance labeled in figure legends. A p-value <0.05 was considered statistically significant.

RESULTS

Opn3 is expressed in retinal ganglion cells and overlaps with OPN4 expression: We used the *Opn3-eGFP* reporter line to assess the expression of the *Opn3* gene in the mouse eye. This reporter was validated by cross-referencing the expression pattern in neural tissue [35] with that of the *Opn3*$^{::mCherry}$ knock-in reporter [47], in which mCherry is fused to the C-terminus of OPN3. High correspondence indicates that *Opn3-eGFP* faithfully reports *Opn3* transcript expression. Although the direct fluorescence of eGFP from this reporter was detectable, we used an anti-eGFP antibody to increase the signal strength.

Table 2. GO/GROW signature genes and primers.

Category	Name	Sequence
Cell surface receptors		
	Drd1	F1: GGTGCTGAAGATTGAAGATCCA
		R1: CGTCCTGACACATGCTGTTATAG
	Drd2	F1: ACCTGTCCTGGTACGATGATG
		R1: GCATGGCATAGTAGTTGTAGTGG
	Gja1/Cx43	F1: ACAGCGGTTGAGTCAGCTTG
		R1: GAGAGATGGGGAAGGACTTGT
	Opn4	F1: GCTTCACAACCAGTCCTGC
		R1: GTCGTGGGGCTAACAGAGAG
	Tgfbr3	F1: GGTGTGAACTGTCACCGATCA
		R1: GTTTAGGATGTGAACCTCCCTTG
Transcription regulators		
	Egrl	F1: ACTTTGCGCCTACAATTCAGG
		R1: AACTTGCCAGGGAATGGAACT
	Fos	F1: TTGAGCGATCATCCCGGTC
		R1: GCGTGAGTCCATACTGGCAAG
	Per2	F1: GAAGACGTGGACATGAGCAGTGGC
		R1: CATCATCAGGGCCTGGGGTGAGTGTT
	Rarb	F1: AGATGACAGCGGAGCTAGAC
		R1: TTCGTGGTGTATTTACCCAGC
	Rxrb	F1: CCACCTCTTACCCCTTCAGC
		R1: TGGAAGAACTGATGACTGGGA
Secreted		
	Bmp2	F1: GCTTCCGTCCCTTTCATTTCT
		R1: AGCCTCCATTTTTGGTAAGGTTT
	Bmp4	F1: TTCCTGGTAACCGAATGCTGA
		R1: CCTGAATCTCGGCGACTTTTT
	Ctgf	F1: GGGCCTCTTCTGCGATTTC
		R1: ATCCAGGCAAGTGCATTGGTA
	Fgf10	F1: TTTGGTGTCTTCGTTCCCTGT
		R1: TAGCTCCGCACATGCCTTC
	IL18	F1: CCTACTTCAGCATCCTCTACTGG
		R1: AGGGTTTCTTGAGAAGGGGAC

Category	Name	Sequence
	Nov	F1: AGTGCCCCAGTATATCACCGA
		R1: GTCACAGGGTCTCATCTCAGA
	Nyx	F1: CCAGGAGTTTCCGTGCGAG
		R1: TGATGAAGGACAGGTTATTGTGG
	Penk	F1: GAGAGCACCAACAATGACGAA
		R1: TCTTCTGGTAGTCCATCCACC
	Sst	F1: ACCGGGAAACAGGAACTGG
		R1: TTGCTGGGTTCGAGTTGGC
	Tgfb1	F1: CTCCCGTGGCTTCTAGTGC
		R1: GCCTTAGTTTGGACAGGATCTG
	Tgfb2	F1: CTTCGACGTGACAGACGCT
		R1: GCAGGGGCAGTGTAAACTTATT
	Vip	F1: AGTGTGCTGTTCTCTCAGTCG
		R1: GCCATTTTCTGCTAAGGGATTCT
MPs/TIMPs		
	Timp1	F1: GCAACTCGGACCTGGTCATAA
		R1: CGGCCCGTGATGAGAAACT
	Timp3	F1: CTTCTGCAACTCCGACATCGT
		R1: GGGGCATCTTACTGAAGCCTC

Molecular Vision 2023; 29:39-57 <http://www.molvis.org/molvis/v29/39>

Retinal ganglion cells (RGCs) were observed to express *Opn3-eGFP* (Figure 1A–C). At birth, *Opn3* expression is observed throughout the ganglion cell layer (identified with the ganglion cell marker RBPMS; Figure 1A, P0.5). However, by P8.5 and P12.5, the proportion of retinal ganglion cells that express *Opn3* had diminished and was restricted to a few cells (Figure 1B,C). Labeling for eGFP at P28 in flat-mount retinas showed a 98.1% overlap with the pan-RGC marker RBPMS (Figure 1D,F). Calbindin and calretinin were found in 42.2% and 20.3% of *Opn3-eGFP* expressing cells, respectively (Figure 1E-G). Interestingly, a significant expression overlap was observed between OPN4 (by antibody labeling) and *Opn3-eGFP* (Figure 1F,G,H), with 23.9% of *Opn3-eGFP* cells immunolabeling for OPN4. OPN4 RGCs have six morphological subtypes with distinct electrophysiological properties and functions [48-53]. Analysis of the morphology of OPN4 immunoreactive cells and the overlapping expression of OPN4 and *Opn3-eGFP* revealed that the M1 subtype that plays a primary role in circadian entrainment and the pupillary light reflex [54] does not express *Opn3* (Figure 1I). However, there is substantial overlap of *Opn3* expression with the M2 and the M4 subtypes of OPN4 RGCs (Figure 1I). The population of OPN4 RGCs, and the M2 subtype specifically (as well as M1 and M3 populations where *Opn3* is not expressed), have been implicated in refractive development and induced myopia responses [27,28]. Outside of the RGCs, *Opn3-eGFP* also showed that *Opn3* is expressed in a distinct layer of cells just outside the retinal pigmented epithelium (RPE, Figure 1A,B,J). These cells are within the choriocapillaris, a vascular component of the choroid that supports the RPE and photoreceptors. *Opn3* choriocapillaris expression increases with development from P0 to P8.5.

Opn3 expression in RGCs does not significantly overlap with expression of neuropsin/Opn5: It has been shown previously that neuropsin/*Opn5* is expressed in retinal ganglion cells [14] and, like OPN4, is involved in the induced myopia response in mice [55]. For this reason, we assessed the relationship between the expression of *Opn3* and *Opn5* in the retina. *Opn5* is expressed at low levels but has been detected successfully using an $Opn5^{cre}$ allele to convert a cre recombinase reporter. Here, we used mice of the genotype $Opn5^{cre}$*;* $Rosa26^{Ai14}$*; Opn3-eGFP* and labeled flat-mount retinas for eGFP and OPN4 (Figure 2A-J). We then assessed 3306 RGCs (n=3 animals) for expression overlap between the three opsins at P28 (Figure 2K,L). This revealed that, of the opsin-expressing RGCs, *Opn5* cells were the most abundant (Figure 2K, L). *Opn5* RGCs rarely showed expression overlap with *Opn3* or OPN4 (Figure 2K,L). However, the significant expression overlap between *Opn3* and OPN4 was confirmed (Figure 2K,L). These data suggested that *Opn5* RGCs were likely to function as a distinct population but that we would need to consider whether the co-expression of *Opn3* and OPN4 might have functional consequences.

Deletion of retinal Opn3 does not influence the number of ipRGCs or OPN4 expression: Our goal of assessing the function of OPN3 in refractive development and induced myopia could be confounded if deletion of *Opn3* in RGCs had an impact on the number of intrinsically photosensitive retinal ganglion cells (ipRGCs) or their expression of OPN4. To assess this, we first confirmed that *mRx-cre* was an effective retinal cre driver by crossing it with the cre reporter *Ai14* and assessing the distribution of tdTomato expressing cells. This showed the expected broad, cre-dependent conversion in retinal neurons (Appendix 1). We then analyzed OPN4 expression in mice with a retina-specific knockout of *Opn3* ($Opn3^{fl/fl}$*; mRx-cre).* In retinae from these animals, we quantified the ipRGC number based on OPN4 immunolabeling in the ganglion cell layer as well as displaced cells in the inner nuclear layer (Appendix 1). A comparison between control and *Opn3* conditional deletion retinae revealed no difference in OPN4 immunoreactivity (Appendix 1) or in the numbers of ipRGCs (Appendix 1). This indicated that despite the existence of *Opn3/Opn4* double-positive RGCs, *Opn3* could be studied independently of *Opn4*.

Opn3 null mice have abnormal eye growth that leads to mild myopia: To assess whether *Opn3* might play a role in refractive development of the eye, we performed ocular biometry and refractive assessment on mice that were *Opn3* germline null ($Opn3^{\Delta Ex2/\Delta Ex2}$). This was performed over a time course between postnatal weeks 3 and 9. Using spectral domain optical coherence tomography (SD-OCT), we measured the depth of the aqueous (Figure 3A), pole-to-pole lens thickness (Figure 3B), corneal thickness (Appendix 2), retinal depth (Appendix 2), choroidal thickness (Appendix 2), vitreous chamber depth (Appendix 2), and the axial length from the outer corneal surface to the RPE–choroid boundary (Figure 3C) [55]. The eyes of both control and *Opn3* null mice are increasing in size over this period, commensurate with postnatal growth.

Biometry assessments showed that the *Opn3* germline null mice had both a reduced aqueous depth (Figure 3A) and a thinner lens (Figure 3B). These dimensional changes accounted completely for the reduced axial length that was also apparent in the *Opn3* null (Figure 3C). Consistent with this, the *Opn3* null did not show any significant change in the thickness of the cornea (Appendix 2), retina (Appendix 2), or choroid (Appendix 3) or in the depth of the vitreous chamber (Appendix 2). The changes to the Opn3 null are summarized

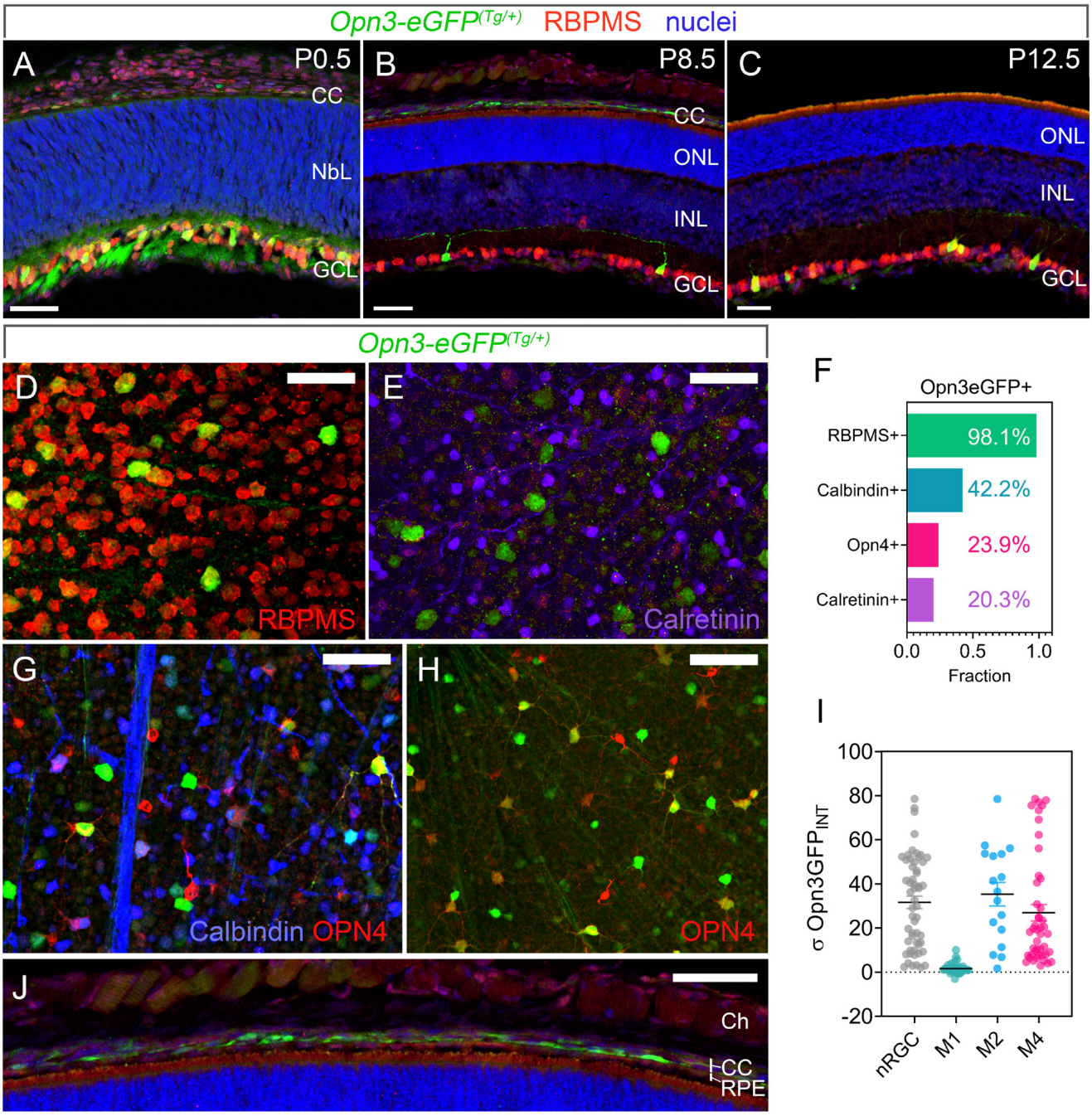

Figure 1. *Opn3* is expressed in retinal ganglion cells. **A**–**C**: Retinal expression of *eGFP* (green) in *Opn3-eGFP*$^{(Tg/+)}$ mice at P0.5 (**A**), P8.5 (**B**), and P12.5 (**C**; 50 µM scale bars), showing expression within RBPMS-labeled (red) retinal ganglion cells (RGCs) in the ganglion cell layer (GCL). Nuclei are DAPI labeled (blue). The proportion of ganglion cells that express *Opn3-eGFP* is high at P0.5 (**A**) and reduced by P8.5 (**B**). *Opn3-eGFP* is also expressed in cells of the choriocapillaris (CC; **A**, **B**). **D**, **E**: Whole-mount retina from *Opn3-eGFP*$^{(Tg/+)}$ mice at P16 labeled for GFP (green) and melanopsin (red; **D**) or GFP (green) calbindin (blue) and calretinin (magenta; 25 µM scale bars). **F**: Chart showing the proportion of *Opn3-eGFP*$^{(Tg/+)}$ cells that are positive for RBPMS (**D**), calretinin (**E**), calbindin (**G**, scale bar 25 µM), and OPN4 (**H**, scale bar 50 µM). **I**: Along with the morphological assessment of dendritic arbors, this analysis identified populations of *Opn3-eGFP* RGCs that did not express OPN4 (nRGC: gray), the M1 subtype of OPN4 RGC, which did not express *Opn3-eGFP* (M1-ipRGC: green), and two subtypes of OPN4 RGC, the M2 (M2-ipRGC: blue) and M4 (M4-ipRGC: red), which expressed both OPN4 and *Opn3-eGFP*. This is represented in the chart showing the relative expression levels of *Opn3-eGFP* in RGCs that do not express OPN4 (nRGCs) as well as the M1, M2, and M4 OPN4 RGCs. (J) Higher magnification image of the Opn3-eGFP labeling in the choriocapillaris (CC). NbL: neuroblastic layer. ONL: outer nuclear layer. INL: inner nuclear layer (50 µM scale bar). RPE: retinal pigment epithelium.

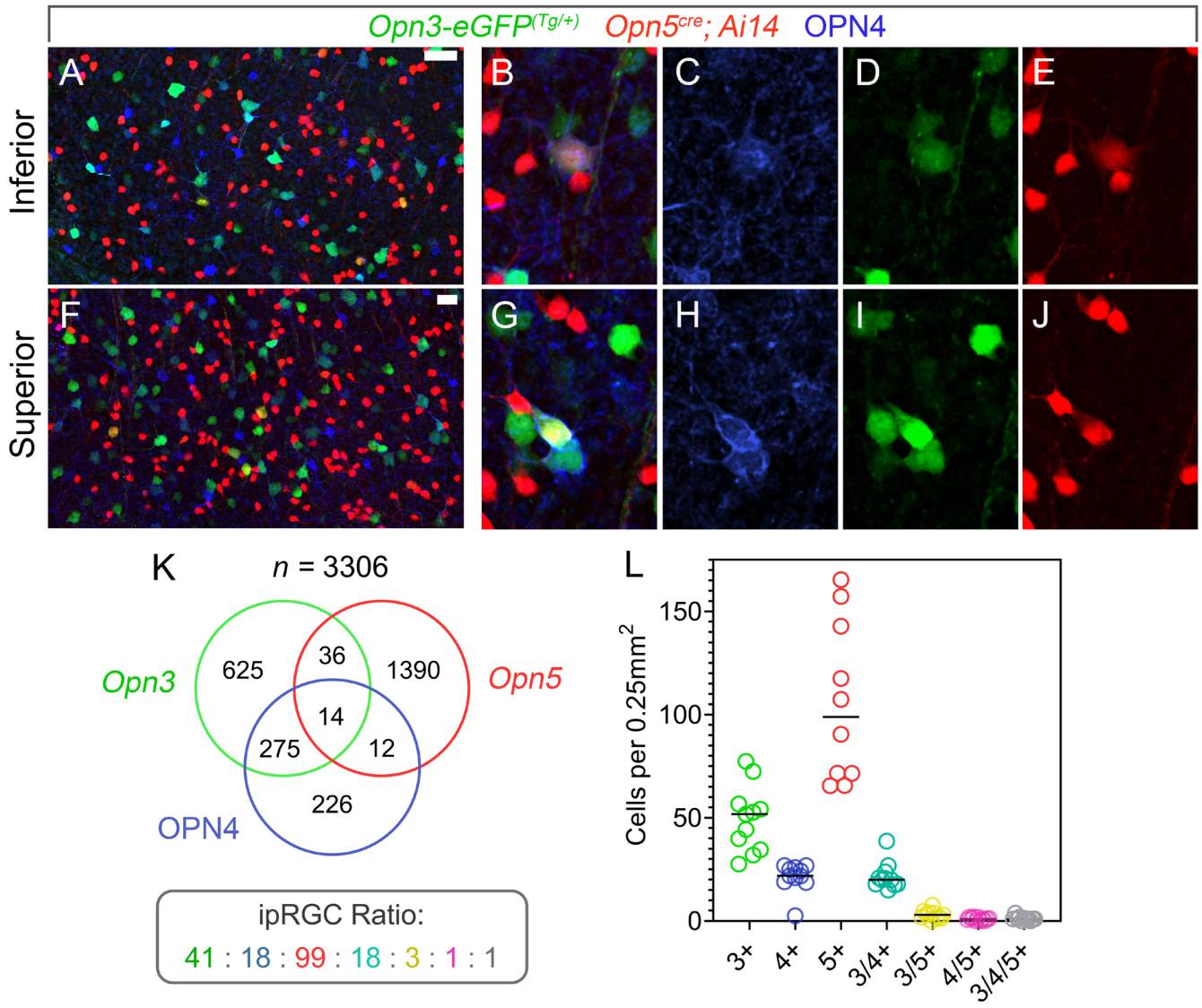

Figure 2. *Opn3*/OPN4 RGCs constitute the largest proportion of multi-opsin RGCs (**A**–**J**). Whole-mount retinae from P28 *Opn3-eGFP; Opn5*^{cre}*; Ai14* mice imaged for GFP (green), OPN4 (blue), and tdTomato (red). Both low (**A**, **F**, 50 µM scale bars) and high (**B**, **G**) magnifications are shown as are the channel separations (**C**–**E** and **H**–**J**). **K**: Venn diagram showing the amount of RGCs, out of 3306 assessed, that express, single, double, or triple combinations of *Opn3*, OPN4, and *Opn5*. These data are also represented in the chart (**L**) showing the opsin expression combinations as a proportion of a single class of opsin-expressing RGCs.

in the chart. These measurements document a role for OPN3 in the development of the anterior eye.

Assessment of the refractive performance of the *Opn3* germline null eye revealed mild myopia (Figure 3D). From 3 to 4 weeks of the time course, the refraction of control eyes increased from −5 to +13 diopters (Figure 3D). In contrast, the refraction of *Opn3* germline null mice increased only slightly from 3 to 5 weeks and then became more negative thereafter. Over the length of the time course, on average, the *Opn3* null showed a reduction in refraction of about −10 diopters by weeks 5–8 (Figure 3D). The mild myopia of the *Opn3* null eye was unexpected because a reduced axial length would normally lead to hyperopia.

The myopia of Opn3 null mice cannot be attributed to retinal OPN3: The process of emmetropization that drives refractive development in the eye is known to be dependent on light detection by photoreceptors [56]. In all cases assessed so far, it is the retinal photoreceptors that mediate light sensing [24,26,27,55,57]. To determine whether the retina was the domain of *Opn3* expression crucial for the phenotype

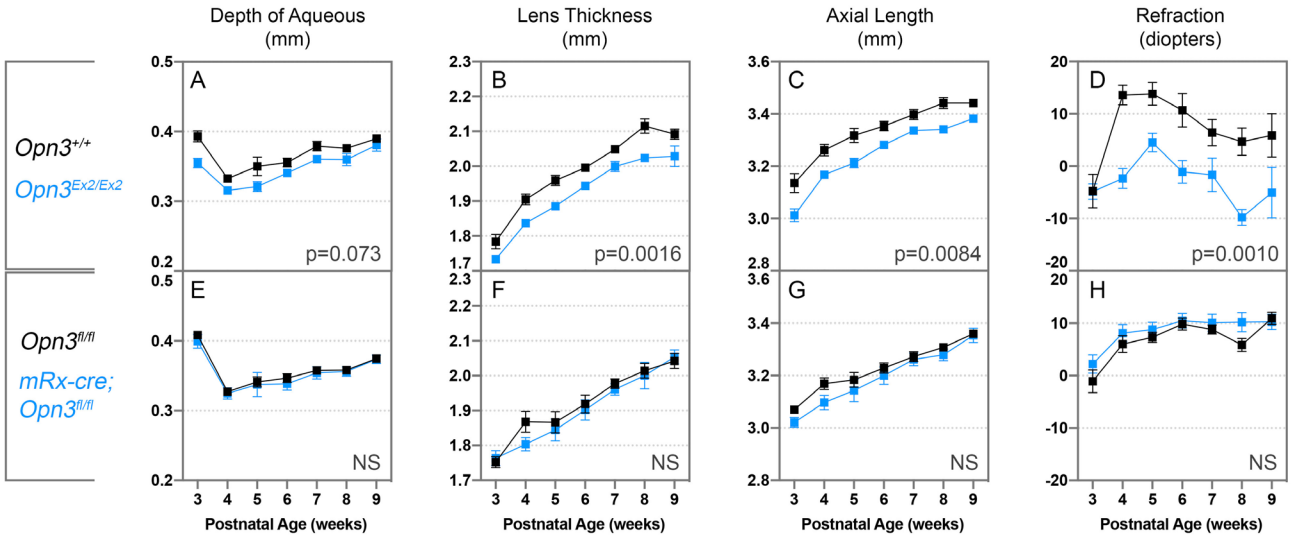

Figure 3. *Opn3* null mice myopic ocular biometry for mice of the *Opn3*$^{Ex2/Ex2}$ (top row) and *Opn3*$^{fl/fl}$*; mRx-cre* genotypes (bottom row), including depth of the aqueous compartment (**A**, **E**), lens thickness (**B**, **F**), axial length (**C**, **G**), and refraction (**D**, **H**). In *Opn3*$^{Ex2/Ex2}$ mice (n=5), the depth of the aqueous is shallower (**A**, blue trace), the lens is thinner (**B**, blue trace), and the axial length is shorter (**C**, blue trace) than in the control *Opn3*$^{+/+}$ cohort (**A**–**C**, black traces, n=4). In addition, *Opn3*$^{Ex2/Ex2}$ mice exhibit significantly reduced refraction (D, blue trace) compared with the control *Opn3*$^{+/+}$ cohort (**D**, black trace). In contrast, no significant changes were observed in these parameters in mice of the *Opn3*$^{fl/fl}$*; mRx-cre* genotype (**E**–**H**, blue traces, n=10) when compared with the *Opn3*$^{fl/fl}$ control cohort (**E**–**H**, black traces, n=11). Statistical significance was assessed using a two-way ANOVA. The p-values in the charts refer to main effect of genotype comparisons. NS: Not significant.

described in the *Opn3* germline null, we generated retinal conditional null mice by combining the *mRx-cre* driver with the *Opn3*^{fl} allele. These generated cohorts of control (*Opn3*$^{fl/fl}$) and experimental (*mRx-cre; Opn3*$^{fl/fl}$) mice were subjected to biometry and refraction as described above. None of the measured features showed any statistically significant change (Figure 3E-H, Appendix 2). This suggests that RGC *Opn3* is not the expression domain that explains the phenotype of the *Opn3* germline null.

Both germline and retina conditional Opn3 null mice are susceptible to induced myopia: The mechanisms underlying myopia pathways can be assessed using induced myopia. Given the refractive development changes observed in *Opn3* null mice, it was interesting to assess their susceptibility to LIM. This analysis was performed using external lenses mounted on a head post according to an established method [21,55,58]. For each mouse, a zero-diopter lens was mounted in front of the control eye (left) and a −30-diopter lens in front of the experimental (right) eye. Lenses were mounted at 3 weeks of age, and biometry and refraction measurements were subsequently taken over a 3-week time course. The analysis was performed for control and experimental cohorts of both germline null (*Opn3*$^{\Delta Ex2/\Delta Ex2}$) and retina conditional null (*mRx-cre; Opn3*$^{fl/fl}$) mice. Data were normalized to the 3 weeks of age time point (t=0) so that the control eye growth response and the experimental eye response to refractive mismatch could be compared.

This analysis showed that *Opn3* germline and conditional mutant mice both responded to the myopiagenic stimulus, albeit with subtle differences. The axial length (Figure 4A, D), corneal thickness (Appendix 3), aqueous depth (Appendix 3), lens thickness (Appendix 3), retinal thickness (Appendix 3), refraction (Figure 4B,E), and choroidal thickness (Figure 3C,F) in cohorts of both *Opn3* mutant genotypes were statistically indistinguishable from control cohorts according to a two-way ANOVA analysis. However, there were notable deviations from controls in some parameters, including a less robust refractive shift and reduced choroidal thinning in *Opn3*$^{\Delta Ex2/\Delta Ex2}$ mice (Figure 4B,C, compare blue and black dashed lines) and retinal change that was thinner in *Opn3*$^{\Delta Ex2/\Delta Ex2}$ mice but thicker in *mRx-cre; Opn3*$^{fl/f}$ mice (Appendix 3 compare blue dashed in D with blue dashed line in H). In summary, loss of function in *Opn3* does not prevent an induced myopia response but appears to subtly change some features of the response.

The myopia GO/GROW myopia gene signature is partly OPN3 dependent: Multiple studies with a variety of animal models have identified a gene signature associated with

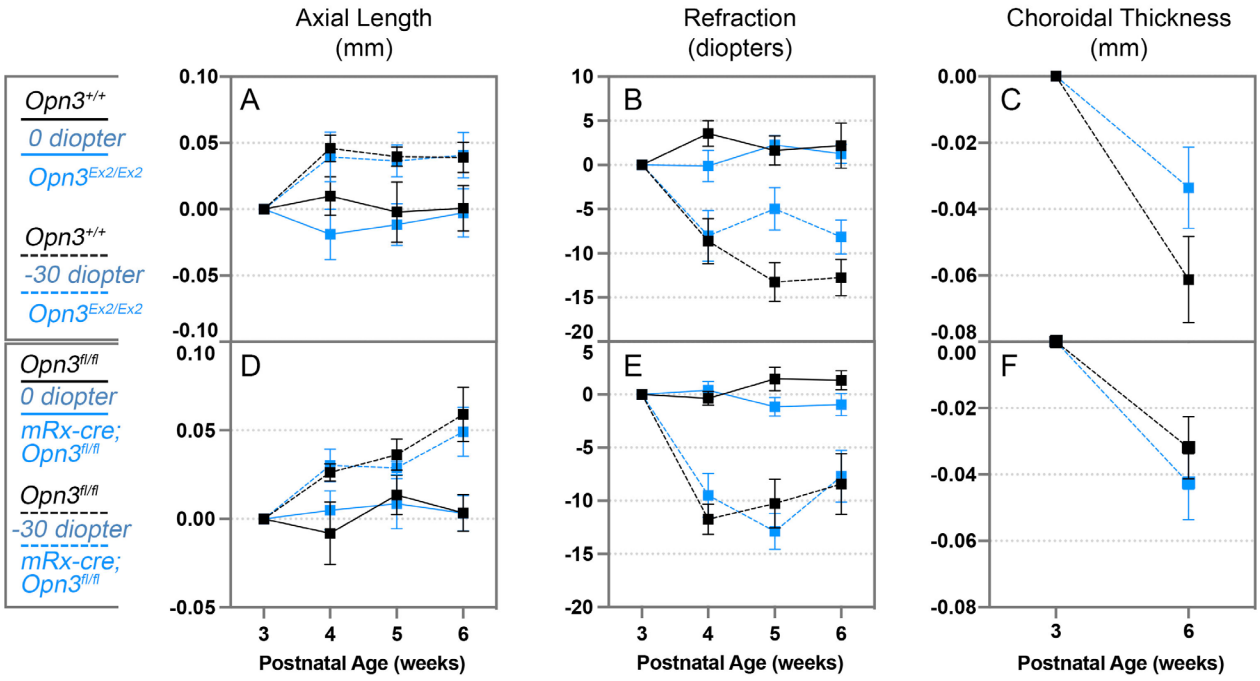

Figure 4. The susceptibility of *Opn3* null mice to LIM is largely unchanged. Relative change in ocular biometry in mice of the *Opn3*$^{Ex2/Ex2}$ (top row) and *Opn3*$^{fl/fl}$*; mRx-cre* genotypes (bottom row) in the LIM model. The data show the change in axial length (**A**, **D**) and refraction (**C**, **F**) when comparing a left eye treated with a 0 diopter lens and a right eye treated with a −30 diopter lens. For choroidal thickness (**C**, **F**), the charts show only the 3-week (t=0) time point compared with the 6-week time point for the right eye, −30 diopter lens. Although the *Opn3*$^{Ex2/Ex2}$ mice showed an apparent reduced susceptibility to choroidal thinning (B, blue and black dashed traces) and refractive shift (**D**, compare blue and black dashed traces), these changes did not reach statistical significance (goggled *Opn3*$^{Ex2/Ex2}$ n=8, goggled control n=8; ungoggled *Opn3*$^{Ex2/Ex2}$ n=5, ungoggled control n=4; goggled *Opn3*$^{fl/fl}$*; mRx-cre* n=10, goggled control n=7; ungoggled *Opn3*$^{fl/fl}$*; mRx-cre* n=10; ungoggled control n=11).

both form-deprivation myopia [59] and LIM [60]. The gene signature, referred to as GO/GROW, is evident in genes that are expressed in the retina [61], RPE [45,62], choroid [63], and sclera [64] and is thought to correspond to the cellular recognition of refractive mismatch and the response in ocular growth. Despite extensive characterization of this gene expression signature in chicks [65-67] and to a lesser degree in guinea pigs [68], tree shrews [69,70], and monkeys [71,72], GO/GROW has not been explored in mice or in the context of genetic models of myopia.

In evaluating the GO/GROW gene signature in this study, we had the dual goals of assessing whether this gene signature was useful in mice and whether any of the genes were *Opn3* dependent. We chose to evaluate a selection of GO/GROW signature genes with a range of functions (transcription factors, secreted factors, membrane proteins; Table 2) at 24 h after myopia induction, a common time point in previous studies using other animal models. We performed this analysis comparing the GO/GROW gene signature in wild-type and *Opn3* null mice, as this was the mutant that demonstrated a unique myopia phenotype and reduced myopic shift in response to LIM.

The analysis showed that some of the GO/GROW signature genes had a distinct response in the *Opn3* null germline (Figure 5A). When compared to the zero-diopter eye, the retina from the −30-diopter eye of *Opn3* null showed a significant downregulation of *Ctgf*/*Ccn2* (Connective Tissue Growth Factor/Cellular Communication Network Factor 2), *Cx43/Gja1* (Connexin 43/Gap Junction A1), and *Egr1* (Early Growth Response 1), with the latter two genes showing a reversed polarity of gene expression change compared with controls (Figure 5A, compare blue and gray bars). An additional group of genes (*Rarb, Penk and Fgf10*) showed a statistical trend in expression change. This analysis indicates that a subset of GO/GROW signature genes are dependent on OPN3 activity for their expression change in response to refractive mismatch.

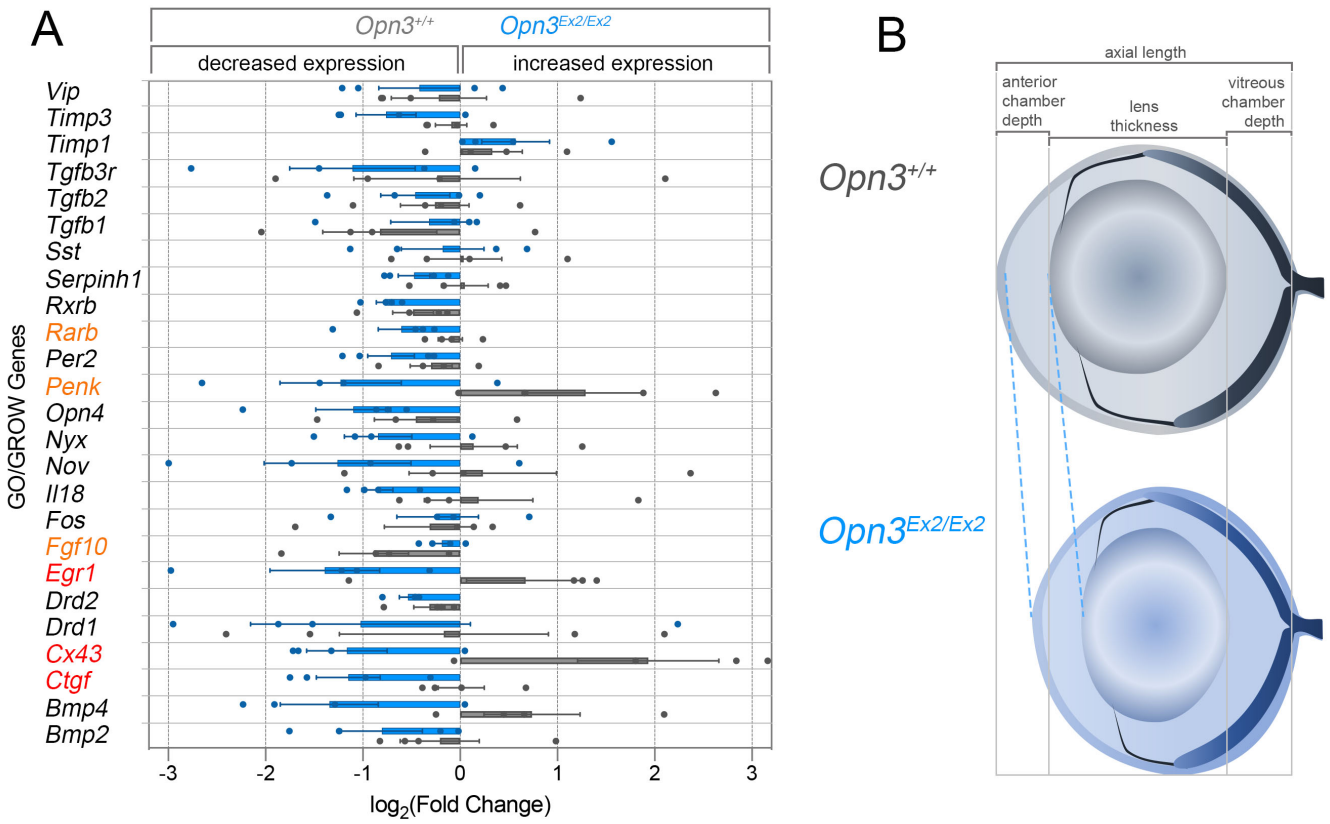

Figure 5. The induced myopia expression of some GO/GROW signature genes is OPN3 dependent. **A**: Chart quantifying changes in the expression of a selection of GO/GROW signature genes in response to a −30-diopter lens in control *Opn3*$^{+/+}$ (gray bars) and experimental *Opn3*$^{Ex2/Ex2}$ (blue bars) mice. Gene expression is shown as $\log_2$ fold change; negative values mean decreased expression, and positive values mean increased expression. **B**: Schematic explaining the changes in eye shape that occur in the Opn3 germline null mice. These include reduced aqueous depth and reduced lens thickness. n=4 for all biologic replicates.

DISCUSSION

Refractive development and induced myopia: The minor role of GWAS-associated genetic variants [73] in the myopia boom [4] and documented environmental risk factors, including outdoor light exposure [74] and focus [75], in myopia development make opsins a prime candidate for the sensors of environmental lighting cues that mediate emmetropization. It is therefore unsurprising that refractive phenotypes have been documented in every opsin signaling pathway studied [23-25], including the non-canonical opsins. Loss of melanopsin/*Opn4* function or of the ipRGCs that express *Opn4* can result in early myopia and late hyperopia [27] or persistent hyperopia [28]. Neuropsin/*Opn5*-dependent violet light stimulation is protective against induced myopia [55] and can explain why sunlight is protective against myopia [74]. Encephalopsin/*Opn3* is widely expressed [32,33,35] but only has a confirmed light-sensing function in adipocytes [17,27,76], with light responses in the colon [77], airway [37], and uterus [38] suggested to be OPN3 dependent. Until this study, the role of *Opn3* in the eye had not been investigated.

We document a myopic phenotype in the germline *Opn3* null that is not present in the retinal conditional null. This phenotype was characterized by short axial length, reduced aqueous compartment depth, and a thinner lens, but preserved vitreous depth, with a reduced axial length resulting from the anterior eye changes. Despite this short axial length, *Opn3* null eyes demonstrate axial elongation in response to the refractive mismatch of LIM, although the resultant myopic shift is less robust than that of the control. The pattern of refractive development and response to LIM in the *Opn3* germline null prompts comparison to refractive development of the *Opn4* null. This been reported by Chakraborty et al. [27] to have a reduced anterior chamber depth abnormal lens placement and, in a Cre/Cre null, to have a shorter axial length [28]. Further, Liu et al. reported that their null had a reduced myopic shift, like the *Opn3* germline null, but with impaired axial elongation.

However, there are also distinct differences between these opsin mutants. Chakraborty et al. [27] reported that the *Opn4* null exhibits slowed axial growth (rather than stable axial length differences) and no differences in lens thickness, resulting in a different refractive phenotype of early myopia and subsequent hyperopia, while Liu's [28] Cre/Cre null is hyperopic throughout development, neither of which match the pattern of the *Opn3* germline null. Further, despite the overlapping expression of *Opn3* and *Opn4* in a proportion of M2 and M4 ipRGCs, the failure of the retina-specific deletion of *Opn3* results in any refractive development phenotype indicates that the crucial domain of *Opn3* expression for this response is not a retinal neuron. Many other domains of *Opn3* expression can be assessed [32,33,35], including the choriocapillaris domain documented here.

Myopia has different classifications based on the source of refractive error. Refractive myopia results from changes in anterior power, while axial myopia results from axial elongation [1]. Many human myopes, however, manifest characteristics of both types [78]. The Reykjavik Eye Study [79] was one of the first studies to report that corneal and lens power characteristics as well as axial length constitute total refractive error, thus underlining the importance of examining myopic progression in its totality. Much of the animal model research on myopia has focused on genetic models or myopia induction models that result in eye elongation, and thus much attention has been focused on axial length. The *Opn3* myopia model highlights the importance of examining ocular dimensions as a whole and provides an animal model for myopia where elongation is not the predominant source of myopic refractive error.

Opn3 germline null animals have a thinner lens, a change that can be associated with myopia development [79-82]. However, when the lens–myopia relationship is explored, an inverse relationship is often found between lens power (correlated with lens thickness) and refractive error/axial length changes in individuals who become myopic earlier in life [83]. For those who develop refractive error later in life, refractive changes are more often a result of changes in anterior focusing, and thus the relationship between lens power and refraction is usually direct [84]. This phenomenon of anterior hyperopia in young myopes is thought to be a counter to myopic axial elongation and has alternatively been explained as an active response to increasing axial length or as a passive mechanical stretching [85], which results in a compensatory reduction in lens power until the lens can no longer compensate [86,87].

However, there is not always a connection between lens thickness and power, as demonstrated by the "lens paradox" of increasing lens thickness over the human lifetime with no corresponding increase in lens power, underlining how changes to both the external structure of the lens (curvature and thickness) and internal refractive gradient influence lens power [84]. As a result, the refraction of a lens is more complicated than its thickness. Some ocular modeling studies have found that both a short anterior chamber [87] as well as, counterintuitively, a thinner, but not posteriorly displaced lens, are both predictive of myopic refraction in the anterior segment [88]. Nonetheless, it is important to consider that most of this research and modeling has been done assuming human eye optics, which may not be generalizable to mice. Further, corneal curvature was not assessed in this study and could be contributing to the overall myopic refraction of the eye.

It is perhaps significant that the features of the *Opn3* germline eye share similarities to myopia of prematurity. Myopia of prematurity results in a shallower anterior eye, a more anteriorly situated lens, and, depending on the study, a shorter axial length. However, myopia of prematurity also involves increased corneal curvature (which we did not assess) and a thicker lens, in contrast to the *Opn3* germline's thinner lens. It is believed that this congenital form of myopia may result from inhibition of anterior eye growth [89-91]. These similarities may suggest that the *Opn3* pathway could be modified in myopia of prematurity.

The GO/GROW gene signature: The GO/GROW gene signature was identified as a response to both form deprivation and LIM in multiple species. In this study, we examined whether GO/GROW gene expression changes could be documented in mice and whether any changes might be dependent on the activity of OPN3. Notably, several the GO/GROW genes, *Ctgf*, *Cx43*, and *Egr1*, all showed significant OPN3-dependent changes in expression 24 h after initiation of a refractive mismatch. Identification of OPN3-dependent GO/GROW gene expression changes will ultimately allow us to better understand the mechanism of action of OPN3 in refractive development.

Ctgf is known to be expressed in the mouse retinal vasculature, specifically vascular endothelial cells, where it works as part of a Hippo pathway regulatory loop to maintain vascular development and blood–retinal barrier function [92] Further, *Ctgf* has also been investigated for its role in binding and inhibition of VEGF, forming what has been called the "fibro-angiogenic switch," which regulates neovascularization after retinal injury [93]. *Ctgf* has been studied in the context of myopia and glaucoma in relation to choroidal neovascularization and the myofibroblastic phenotype with increased ECM deposition seen in severe disease [94,95].

In a previously published study on the retinal GO-GROW signature in tree shrews, *Ctgf* expression was found to be significantly downregulated in response to myopia induction after 6 h, following the trend of our *Opn3* mutants [96].

The connection of *CX43* to myopia has also been documented, particularly in a clinical context, as missense mutations in the gap junction gene are known to cause oculodentaldigital displasia, which results in a spectrum of disease affecting the teeth, limbs, eye, and ocular adnexa [97]. Various ocular phenotypes have been reported with these mutations, including syndromic myopia with a short axial length, a shallow anterior chamber, and glaucoma [98]. *Cx43* has also been a candidate gap junction in studies on the transmission of epigenetic signals through siRNA as a mediator of neuronal regeneration and modulation, and it was found to have a unique ability to transmit 12–24 nucleotide-long sequences when compared to *Cx32* and *Cx26* [99]. This has been suggested as a potential mode of transmission for cellular response to myopia development as well as other diseases, including retinal vascular disease, macular degeneration, and retinal damage in traumatic brain injury (TBI), the last of which is characterized by *Cx43* downregulation [100].

Egr1/*Zenk* has long been the subject of interest in myopia research since it was first identified in chicks [101] as an immediate early gene response to goggling. *Egr1*/Zenk is upregulated under induced hyperopia and downregulated under induced myopia [102]. Later, along with the *nob* (*Nyx* null) mouse model [103], the *Egr1* null became one of the first genetic models of mouse myopia [104]. *Opn3* null downregulation of *Egr1* therefore follows the induced myopia pattern seen in these previous studies as well as that reported after 6 h in the study by He et al. [45]

Conclusions: This analysis shows that the opsin family GPCR encephalopsin/OPN3 is required for normal refractive development of the eye and that a non-retinal domain of expression is involved. The analysis also shows that several of the GO/GROW refractive mismatch signature genes are changed in an OPN3-dependent manner. Thus, this work identifies the role of opsin family GPCR encephalopsin/OPN3 in refractive development and the response to refractive mismatch. This work adds OPN3 to the list of opsin family GPCRs (in the mouse, OPN4 [27,28], OPN5 [55], the cone opsin (OPN1SW/OPN1MW) pathways [26], and OPN2 [24]) that are implicated in emmetropization and myopia. The exclusion of retinal *Opn3*, a domain crucial for the refractive development phenotype, suggests a distinct mechanism of involvement of the other opsins. Future work could address this question as well as the molecular mechanism of action of OPN3, including an investigation of the light dependence of this phenotype and the developmental periods of refractive development that require OPN3.

APPENDIX 1. CONDITIONAL DELETION OF RETINAL *OPN3* DOES NOT ALTER OPN4 RGCS NUMBERS.

To access the data, click or select the words "Appendix 1."

APPENDIX 2. SHORTENED $OPN3^{EX2/EX2}$ AXIAL LENGTH IS NOT PROGRESSIVE.

To access the data, click or select the words "Appendix 2."

APPENDIX 3. LENS INDUCED MYOPIA FOR $OPN3^{EX2/EX2}$ AND MRX-CRE; $OPN3^{FL/FL}$ INDUCES NO CHANGES IN THE CORNEA, DEPTH OF THE AQUEOUS COMPARTMENT, LENS, AND RETINA.

To access the data, click or select the words "Appendix 3."

ACKNOWLEDGMENTS

We thank P. Speeg for mouse colony management. This work was supported by National Institutes of Health grants R01EY032029, R01EY032752, R01EY032566, as well as funds from the McClung Foundation, the CCHMC Gap/RIP Funding Program and Academic and Research Committee, to R.A.L. and NIGMS 5T32GM063483 to UC MSTP, funds from the Goldman Chair of the Abramson Pediatric Eye Institute at CCHMC, and Japan Agency for Medical Research and Development (AMED) under Grant Number JP22 gm1510007 to T.K. Data were previously presented in the 2023 ISER Conference in Gold Coast, Australia. Contributions: C.L. and R.A.L. conceived and directed the study. M.T.P. played a senior advisory role. C.L. performed the refractive assessments, RT-qPCR, and mouse biometry quantification. C.L and K.Y.M. performed the head pedestal surgery and lens induced myopia measurements. C.L and S.V. performed the tissue preparation for the RT-qPCR experiments to ensure prompt isolation of tissues to minimize circadian variability. SD performed the assessment of *Opn3* expression in the eye, *Opn3* retinal ganglion cell subtype identification, and mRx-Cre retinal ganglion cell quantification. K.Z. wrote the MatLab program to analyze choroidal thickness and assisted with technical assistance. T.K and K.T. provided the mouse spectacles from their laboratory which H.J shipped to us. Additionally, H.J. and X.J developed the protocol for mouse lens induced myopia and H.J. provided technical assistance. M.T.P. provided assistance in establishing the protocols for refractive and mouse biometric assessment and statistical

analysis along with her student, D.B. Additionally, D.B. provided technical assistance with the Bioptogen OCT and Stria-Tech Photorefractor and wrote the MatLab program MouseSwimmer to quantify ocular measurements. C.L. and R.A.L wrote the manuscript and R.A.L. provided coordinating project leadership. Communication should be directed to R. A. L. Division of Pediatric Ophthalmology, Cincinnati Children's Hospital Medical Center, 3333 Burnet Avenue, Cincinnati OH 45,229, Tel: 513–636–2700 (Office), 513–803–2230 (Assistant), Fax: 513–636–4317. Email: richard.lang@cchmc.org Ethics declarations: The Lang laboratory participates in a sponsored research agreement between CCHMC and BIOS Lighting, Inc. Kazuo Tsubota reports his position as CEO of Tsubota Laboratory, Inc., Tokyo, Japan, a company producing myopia-related devices. The Lang laboratory participates in a sponsored research agreement between CCHMC and BIOS Lighting, Inc.

REFERENCES

1. Flitcroft DI, He M, Jonas JB, Jong M, Naidoo K, Ohno-Matsui K. Rahi J, Resnikoff S, Vitale S, Yannuzzi LIMI – Defining and classifying myopia: A proposed set of standards for clinical and epidemiologic studies. Invest Ophthalmol Vis Sci 2019; 60:M20-30. [PMID: 30817826].
2. Holden BA, Jong M, Davis S, Wilson D, Fricke T, Resnikoff S. Nearly 1 billion myopes at risk of myopia-related sight-threatening conditions by 2050 - time to act now. Clin Exp Optom 2015; 98:491-3. [PMID: 26769175].
3. Hashemi H, Fotouhi A, Yekta A, Pakzad R, Ostadimoghaddam H, Khabazkhoob M. Global and regional estimates of prevalence of refractive errors: Systematic review and meta-analysis. J Curr Ophthalmol [Internet] 2018; 30:3-22. [PMID: 29564404].
4. Holden BA, Fricke TR, Wilson DA, Jong M, Naidoo KS, Sankaridurg P, Wong TY, Naduvilath TJ, Resnikoff S. Global Prevalence of Myopia and High Myopia and Temporal Trends from 2000 through 2050. Ophthalmology 2016; 123:1036-42. .
5. Gwiazda J. Treatment Options of Myopia. Changes 2012; 29:997-1003. .
6. Wong TY, Ferreira A, Hughes R, Carter G, Mitchell P. Epidemiology and disease burden of pathologic myopia and myopic choroidal neovascularization: An evidence-based systematic review. Am J Ophthalmol 2014; 157:1-47. [PMID: 24099276].
7. Tedja MS, Wojciechowski R, Hysi PG, Eriksson N, Furlotte NA, Verhoeven VJM, Iglesias AI, Meester-Smoor MA, Tompson SW, Fan Q, Khawaja AP, Cheng CY, Höhn R, Yamashiro K, Wenocur A, Grazal C, Haller T, Metspalu A, Wedenoja J, Jonas JB, Wang YX, Xie J, Mitchell P, Foster PJ, Klein BEK, Klein R, Paterson AD, Hosseini SM, Shah RL, Williams C, Teo YY, Tham YC, Gupta P, Zhao W, Shi Y, Saw WY, Tai ES, Sim XL, Huffman JE, Polašek O, Hayward C, Bencic G, Rudan I, Wilson JF. CREAM Consortium; 23andMe Research Team; UK Biobank Eye and Vision Consortium; Joshi PK, Tsujikawa A, Matsuda F, Whisenhunt KN, Zeller T, van der Spek PJ, Haak R, Meijers-Heijboer H, van Leeuwen EM, Iyengar SK, Lass JH, Hofman A, Rivadeneira F, Uitterlinden AG, Vingerling JR, Lehtimäki T, Raitakari OT, Biino G, Concas MP, Schwantes-An TH, Igo RP Jr, Cuellar-Partida G, Martin NG, Craig JE, Gharahkhani P, Williams KM, Nag A, Rahi JS, Cumberland PM, Delcourt C, Bellenguez C, Ried JS, Bergen AA, Meitinger T, Gieger C, Wong TY, Hewitt AW, Mackey DA, Simpson CL, Pfeiffer N, Pärssinen O, Baird PN, Vitart V, Amin N, van Duijn CM, Bailey-Wilson JE, Young TL, Saw SM, Stambolian D, MacGregor S, Guggenheim JA, Tung JY, Hammond CJ, Klaver CCW. Genome-wide association meta-analysis highlights light-induced signaling as a driver for refractive error. Nat Genet 2018; 50:834-48. .
8. Hysi PG, Choquet H, Khawaja AP, Wojciechowski R, Tedja MS, Yin J, Simcoe MJ, Patasova K, Mahroo OA, Thai KK, Cumberland PM, Melles RB, Verhoeven VJM, Vitart V, Segre A, Stone RA, Wareham N, Hewitt AW, Mackey DA, Klaver CCW, MacGregor S. Consortium for Refractive Error and Myopia. Khaw PT, Foster PJ; UK Eye and Vision Consortium; Guggenheim JA; 23andMe Inc.; Rahi JS, Jorgenson E, Hammond CJ. Meta-analysis of 542,934 subjects of European ancestry identifies new genes and mechanisms predisposing to refractive error and myopia. Nat Genet 2020; 52:401-7. .
9. Ang M, Wong TY. Updates on myopia: A clinical perspective. Springer Singapore; 2020;1–305.
10. Muralidharan AR, Lança C, Biswas S, Barathi VA, Wan Yu Shermaine L, Seang-Mei S, Milea D, Najjar RP. Light and myopia: from epidemiological studies to neurobiological mechanisms. Ther Adv Ophthalmol. 2021; 13:251584142110592-.
11. Dharani R, Lee CF, Theng ZX, Drury VB, Ngo C, Sandar M, Wong TY, Finkelstein EA, Saw SM. Comparison of measurements of time outdoors and light levels as risk factors for myopia in young Singapore children. Eye (Basingstoke) 2012; 26:911-8. .
12. Ho CL, Wu WF, Liou YM. Dose-response relationship of outdoor exposure and myopia indicators: A systematic review and meta-analysis of various research methods. Int J Environ Res Public Health 2019; 16:2595[PMID: 31330865].
13. Wallman J, Winawer J. Homeostasis of eye growth and the question of myopia. Neuron 2004; 43:447-68. [PMID: 15312645].
14. Buhr ED, Yue WWS, Ren X, Jiang Z, Liao HWR, Mei X. Neuropsin (OPN5)-mediated photoentrainment of local circadian oscillators in mammalian retina and cornea. Proc Natl Acad Sci USA 2015; 112:201516259-[PMID: 26392540].
15. Rao S, Chun C, Fan J, Kofron JM, Yang MB, Hegde RS, Ferrara N, Copenhagen DR, Lang RA. A direct and melanopsin-dependent fetal light response regulates mouse eye development. Nature 2013; 494:243-6. .

16. Buhr ED, Vemaraju S, Diaz N, Lang RA, Van Gelder RN. Neuropsin (OPN5) Mediates Local Light-Dependent Induction of Circadian Clock Genes and Circadian Photoentrainment in Exposed Murine Skin. Curr Biol 2019; 29:3478-3487.e4. [PMID: 31607531].

17. Nayak G, Zhang KX, Vemaraju S, Odaka Y, Buhr ED, Holt-Jones A, Kernodle S, Smith AN, Upton BA, D'Souza S, Zhan JJ, Diaz N, Nguyen MT, Mukherjee R, Gordon SA, Wu G, Schmidt R, Mei X, Petts NT, Batie M, Rao S, Hogenesch JB, Nakamura T, Sweeney A, Seeley RJ, Van Gelder RN, Sanchez-Gurmaches J, Lang RA. Adaptive Thermogenesis in Mice Is Enhanced by Opsin 3-Dependent Adipocyte Light Sensing. Cell Reports 2020; 30:672-686. .

18. Zhang KX, D'Souza S, Upton BA, Kernodle S, Vemaraju S, Nayak G, Gaitonde KD, Holt AL, Linne CD, Smith AN, Petts NT, Batie M, Mukherjee R, Tiwari D, Buhr ED, Van Gelder RN, Gross C, Sweeney A, Sanchez-Gurmaches J, Seeley RJ, Lang RA. Violet-light suppression of thermogenesis by opsin 5 hypothalamic neurons. Nature 2020; 585:420-5. .

19. Schaeffel F. Test systems for measuring ocular parameters and visual function in mice. Front Biosci 2008; 13:4904-11. .

20. Troilo D, Smith EL, Nickla DL, Ashby R. Tkatchenko A v., Ostrin LA, et alImi – Report on experimental models of emmetropization and myopia. Invest Ophthalmol Vis Sci 2019; 60:M31-88. [PMID: 30817827].

21. Tkatchenko TV, Shen Y, Tkatchenko AV. Mouse experimental myopia has features of primate myopia. Invest Ophthalmol Vis Sci 2010; 51:1297-303. .

22. Chakraborty R, Pardue MT. Molecular and Biochemical aspects of the retina on refraction. Prog Mol Biol Transl Sci 2015; 134:249-67. [PMID: 26310159].

23. . Park H na. Jabbar SB, Tan CC, Sidhu CS, Abey J, Aseem F, et alVisually-driven ocular growth in mice requires functional rod photoreceptors. Invest Ophthalmol Vis Sci 2014; 55:6272-9. [PMID: 25183765].

24. Mohanty P, Brown D, Mazade R, Pardue MT. Rod pathway signaling has protective effects on myopia susceptibility in dim, but not bright light. Invest Ophthalmol Vis Sci 2021; 62:1395-.

25. Hagen LA, Arnegard S, Kuchenbecker JA, Gilson SJ, Neitz M, Neitz J, Baraas RC. The association between L:M cone ratio, cone opsin genes and myopia susceptibility. Vision Res 2019; 162:20-8. .

26. Chakraborty R, Yang V, Park HN, Landis EG, Dhakal S, Motz CT, Bergen MA, Iuvone PM, Pardue MT. Lack of cone mediated retinal function increases susceptibility to form-deprivation myopia in mice. Exp Eye Res 2019; 180:226-30. .

27. Chakraborty R, Landis EG, Mazade R, Yang V, Strickland R, Hattar S, Stone RA, Iuvone PM, Pardue MT. Melanopsin modulates refractive development and myopia. Exp Eye Res 2022; 214:108866-.

28. Liu AL, Liu YF, Wang G, Shao YQ, Yu CX, Yang Z, Zhou ZR, Han X, Gong X, Qian KW, Wang LQ, Ma YY, Zhong YM, Weng SJ, Yang XL. The role of ipRGCs in ocular growth and myopia development. Sci Adv 2022; 8:eabm9027-.

29. Jiang X, Pardue MT, Mori K, Ikeda SI, Torii H, D'Souza S, Lang RA, Kurihara T, Tsubota K. Violet light suppresses lens-induced myopia via neuropsin (OPN5) in mice. Proc Natl Acad Sci USA 2021; 118:1-8. .

30. Koyanagi M, Takada E, Nagata T, Tsukamoto H, Terakita A. Homologs of vertebrate Opn3 potentially serve as a light sensor in nonphotoreceptive tissue. Proc Natl Acad Sci USA 2013; 110:4998-5003. [PMID: 23479626].

31. Sugihara T, Nagata T, Mason B, Koyanagi M, Terakita A. Absorption characteristics of vertebrate non-visual opsin, Opn3. PLoS One 2016; 11:1-15. [PMID: 27532629].

32. Blackshaw S, Snyder SH. Encephalopsin: A novel mammalian extraretinal opsin discretely localized in the brain. J Neurosci 1999; 19:3681-90. [PMID: 10234000].

33. Halford S, Freedman MS, Bellingham J, Inglis SL, Poopalasundaram S, Soni BG, Foster RG, Hunt DM. Characterization of a novel human opsin gene with wide tissue expression and identification of embedded and flanking genes on chromosome 1q43. Genomics 2001; 72:203-8. .

34. Tsuchiya S, Buhr ED, Higashide T, Sugiyama K, van Gelder RN. Light entrainment of the murine intraocular pressure circadian rhythm utilizes non-local mechanisms. PLoS One 2017; 12:1-12. [PMID: 28934261].

35. Davies WIL, Sghari S, Upton BA, Nord C, Hahn M, Ahlgren U, Lang RA, Gunhaga L. Distinct opsin 3 (Opn3) expression in the developing nervous system during mammalian embryogenesis. eNeuro 2021; 8:1-18. .

36. Sato M, Tsuji T, Yang K, Ren X, Dreyfuss JM, Huang TL. Cell-autonomous light sensitivity via Opsin3 regulates fuel utilization in brown adipocytes. PLoS Biol 2020; 18:e3000630-[PMID: 32040503].

37. Wu AD, Dan W, Zhang Y, Vemaraju S, Upton BA, Lang RA, Buhr ED, Berkowitz DE, Gallos G, Emala CW, Yim PD. Opsin 3–Gas promotes airway smooth muscle relaxation modulated by G protein receptor kinase 2. Am J Respir Cell Mol Biol 2021; 64:59-68. .

38. Yim PD, Hyuga S, Wu AD, Dan W, Vink JY, Gallos G. Activation of an Endogenous Opsin 3 Light Receptor Mediates Photo-Relaxation of Pre-Contracting Late Gestation Human Uterine Smooth Muscle Ex Vivo. Reprod Sci 2020; 27:1791-801. [PMID: 32166706].

39. Olinski LE, Lin EM, Oancea E. Illuminating insights into opsin 3 function in the skin. Adv Biol Regul 2020; 75:1-12. .

40. Klimova L, Lachova J, Machon O, Sedlacek R, Kozmik Z. Generation of mRx-Cre Transgenic Mouse Line for Efficient Conditional Gene Deletion in Early Retinal Progenitors. PLoS One 2013; 8:1-6[PMID: 23667567].

41. Alizadeh A, Clark J, Seeberger T, Hess J, Blankenship T, FitzGerald PG. Characterization of a mutation in the lens-specific CP49 in the 129 strain of mouse. Invest Ophthalmol Vis Sci 2004; 45:884-91. [PMID: 14985306].

42. Nguyen MT, Vemaraju S, Nayak G, Odaka Y, Buhr ED, Alonzo N, Tran U, Batie M, Upton BA, Darvas M, Kozmik Z, Rao S, Hegde RS, Iuvone PM, Van Gelder RN, Lang RA. An opsin 5–dopamine pathway mediates light-dependent vascular development in the eye. Nat Cell Biol 2019; 21:420-9. .

43. D'Souza SP, Swygart DI, Wienbar SR, Upton BA, Zhang KX, Mackin RD, Casasent AK, Samuel MA, Schwartz GW, Lang RA. Retinal patterns and the cellular repertoire of neuropsin (Opn5) retinal ganglion cells. J Comp Neurol 2022; 530:1247-62. .

44. Tkatchenko TV, Shah RL, Nagasaki T, Tkatchenko AV. Analysis of genetic networks regulating refractive eye development in collaborative cross progenitor strain mice reveals new genes and pathways underlying human myopia. BMC Med Genomics 2019; 12:1-24. [PMID: 31362747].

45. He L, Frost MR, Siegwart JT Jr, Norton TT. Altered gene expression in tree shrew retina and retinal pigment epithelium produced by short periods of minus-lens wear. Exp Eye Res 2018; 168:77-88. [PMID: 29329973].

46. Spandidos A, Wang X, Wang H, Seed B. PrimerBank: A resource of human and mouse PCR primer pairs for gene expression detection and quantification. Nucleic Acids Res 2009; 38:SUPPL.1792-9. [PMID: 19906719].

47. Olinski LE, Tsuda AC, Kauer JA, Oancea E. Endogenous opsin 3 (Opn3) protein expression in the adult brain using a novel opn3-mcherry knock-in mouse model. eNeuro 2020; 7:1-19. [PMID: 32737180].

48. Schmidt TM, Taniguchi K, Kofuji P. Intrinsic and extrinsic light responses in melanopsin-expressing ganglion cells during mouse development. J Neurophysiol 2008; 100:371-84. [PMID: 18480363].

49. Schmidt TM, Kofuji P. Differential cone pathway influence on intrinsically photosensitive retinal ganglion cell subtypes. J Neurosci 2010; 30:16262-71. [PMID: 21123572].

50. Schmidt TM, Alam NM, Chen S, Kofuji P, Li W, Prusky GT, Hattar S. A Role for Melanopsin in Alpha Retinal Ganglion Cells and Contrast Detection. Neuron 2014; 82:781-8. Internet[PMID: 24853938].

51. Quattrochi LE, Stabio ME, Kim I, Ilardi MC, Michelle Fogerson P, Leyrer ML, Berson DM. The M6 cell: A small-field bistratified photosensitive retinal ganglion cell. J Comp Neurol 2019; 527:297-311. .

52. Schmidt TM, Kofuji P. Structure and Function of Bistratified Intrinsically Photosensitive Retinal Ganglion Cells in the Mouse Tiffany. J Comp Neurol 2011; 519:1492-504. [PMID: 21452206].

53. Stabio ME, Sabbah S, Quattrochi LE, Ilardi MC, Fogerson PM, Leyrer ML, Kim MT, Kim I, Schiel M, Renna JM, Briggman KL, Berson DM. The M5 Cell: A Color-Opponent Intrinsically Photosensitive Retinal Ganglion Cell. Neuron 2018; 97:150-63. .

54. Chen SK, Badea TC, Hattar S. Photoentrainment and pupillary light reflex are mediated by distinct populations of ipRGCs. Nature 2011; 476:92-6. [PMID: 21765429].

55. Jiang X, Pardue MT, Mori K, Ikeda SI, Torii H, D'Souza S, Lang RA, Kurihara T, Tsubota K. Violet light suppresses lens-induced myopia via neuropsin (OPN5) in mice. Proc Natl Acad Sci USA 2021; 118:1-8. .

56. Wallman J, Winawer J. Homeostasis of eye growth and the question of myopia. Neuron 2004; 43:447-68. [PMID: 15312645].

57. Hagen LA, Arnegard S, Kuchenbecker JA, Gilson SJ, Neitz M, Neitz J, Baraas RC. The association between L:M cone ratio, cone opsin genes and myopia susceptibility. Vision Res 2019; 162:20-8. .

58. Faulkner AE, Kim MK, Iuvone PM, Pardue MT. Head-mounted goggles for murine form deprivation myopia. J Neurosci Methods 2007; 161:96-100. [PMID: 17126909].

59. Morgan I, Kucharski R, Krongkaew N, Firth SI, Megaw P, Maleszka R. Screening for differential gene expression during the development of form-deprivation myopia in the chicken. Optom Vis Sci 2004; 81:148-55. [PMID: 15127934].

60. Guo L, Frost MR, He L, Siegwart JT, Norton TT. Gene expression signatures in tree shrew sclera in response to three myopiagenic conditions. Invest Ophthalmol Vis Sci 2013; 54:6806-19. [PMID: 24045991].

61. Tkatchenko AV, Walsh PA, Tkatchenko TV, Gustincich S, Raviola E. Form deprivation modulates retinal neurogenesis in primate experimental myopia. Proc Natl Acad Sci USA 2006; 103:4681-6. .

62. Zhang Y, Raychaudhuri S, Wildsoet CF. Imposed optical defocus induces isoform-specific up-regulation of TGFβ gene expression in chick retinal pigment epithelium and choroid but not neural retina. PLoS One 2016; 11:1-15. .

63. He L, Frost MR, Siegwart JT, Norton TT. Gene expression signatures in tree shrew choroid during lens-induced myopia and recovery. Exp Eye Res 2014; 123:56-71. [PMID: 24742494].

64. Srinivasalu N, McFadden SA, Medcalf C, Fuchs L, Chung J, Philip G, Richardson A, Riaz M, Baird PN. Gene expression and pathways underlying form deprivation myopia in the Guinea pig sclera. Invest Ophthalmol Vis Sci 2018; 59:1425-34. .

65. Ohngemach S, Buck C, Simon P, Schaeffel F, Feldkaemper M. Temporal changes of novel transcripts in the chicken retina following imposed defocus. Mol Vis 2004; 10:1019-27. [PMID: 15635295].

66. McGlinn AM. Baldwin2 DA, Tobias3 JW, Budak MT, Khurana TS, Stone RA. Form-Deprivation Myopia in Chick Induces Limited Changes in Retinal Gene Expression. Invest Ophthalmol Vis Sci 2007; 48:1-12. [PMID: 17197509].

67. Riddell N, Giummarra L, Hall NE, Crewther SG. Bidirectional expression of metabolic, structural, and immune pathways in early myopia and hyperopia. Front Neurosci 2016; 10:1-16. [PMID: 27625591].

68. Goto S, Muroy SE, Zhang Y, Saijo K, Kolora SRR, Zhu Q, Wildsoet CF. Gene Expression Signatures of Contact

Lens-Induced Myopia in Guinea Pig Retinal Pigment Epithelium. Invest Ophthalmol Vis Sci 2022; 63:1-3. .

69. Guo L, Frost MR, Siegwart JT, Norton TT. Gene expression signatures in tree shrew sclera during recovery from minus-lens wear and during plus-lens wear. Mol Vis 2019; 25:311-28. [PMID: 31341380].

70. Ku H, Chen JJ, Hu M, Tien PT, Lin HJ, Xu G, Wan L, Gan D. Myopia Development in Tree Shrew Is Associated with Chronic Inflammatory Reactions. Curr Issues Mol Biol 2022; 44:4303-13. .

71. Lambert SR, Fernandes A, Haque R, Smith EL, Iuvone PM. Gene Expression Associated with Lens–Induced Myopia in Rhesus Monkeys. Invest Ophthalmol Vis Sci 2004; 45:1161-.

72. Tkatchenko TV, Troilo D, Benavente-Perez A, Tkatchenko AV. Gene expression in response to optical defocus of opposite signs reveals bidirectional mechanism of visually guided eye growth. PLoS Biol 2018; 16:1-26. .

73. Hysi PG, Wojciechowski R, Rahi JS, Hammond CJ. Genome-wide association studies of refractive error and myopia, lessons learned, and implications for the future. Invest Ophthalmol Vis Sci 2014; 55:3344-51. [PMID: 24876304].

74. Ho CL, Wu WF, Liou YM. Dose-response relationship of outdoor exposure and myopia indicators: A systematic review and meta-analysis of various research methods. Int J Environ Res Public Health 2019; 16:1-17[PMID: 31330865].

75. Wen L, Cao Y, Cheng Q, Li X, Pan L, Li L, Zhu H, Lan W, Yang Z. Objectively measured near work, outdoor exposure and myopia in children. Br J Ophthalmol 2020; 104:1542-7. .

76. Ondrusova K, Fatehi M, Barr A, Czarnecka Z, Long W, Suzuki K, Campbell S, Philippaert K, Hubert M, Tredget E, Kwan P, Touret N, Wabitsch M, Lee KY, Light PE. Subcutaneous white adipocytes express a light sensitive signaling pathway mediated via a melanopsin/TRPC channel axis. Sci Rep 2017; 7:1-9. .

77. Dan W, Park GH, Vemaraju S, Wu AD, Perez K, Rao M. Light-Mediated Inhibition of Colonic Smooth Muscle Constriction and Colonic Motility via Opsin 3. Front Physiol 2021; 12:744294[PMID: 34975518].

78. Ludwig CA, Shields RA, Chen TA, Powers MA, Wilkin Parke D 3rd, Moshfeghi AA, Moshfeghi DM. A novel classification of high myopia into anterior and posterior pathologic subtypes. Graefes Arch Clin Exp Ophthalmol 2018; 256:1847-56. .

79. Olsen T, Arnarsson A, Sasaki H, Sasaki K, Jonasson F. On the ocular refractive components: The Reykjavik Eye Study. Acta Ophthalmol Scand 2007; 85:361-6. [PMID: 17286626].

80. Zadnik K, Mutti DO, Fusaro RE, Adams AJ. Longitudinal evidence of crystalline lens thinning in children. Invest Ophthalmol Vis Sci 1995; 36:1581-7. [PMID: 7601639].

81. Muralidharan G, Martínez-Enríquez E, Birkenfeld J, Velasco-Ocana M, Pérez-Merino P, Marcos S. Morphological changes of human crystalline lens in myopia. Biomed Opt Express 2019; 10:6084-[PMID: 31853387].

82. Mutti DO, Mitchell GL, Sinnott LT, Jones-Jordan LA, Moeschberger ML, Cotter SA, Kleinstein RN, Manny RE, Twelker JD, Zadnik K. CLEERE Study Group. Corneal and crystalline lens dimensions before and after myopia onset. Optom Vis Sci 2012; 89:251-62. .

83. Iribarren R, Morgan IG, Nangia V, Jonas JB. Crystalline lens power and refractive error. Invest Ophthalmol Vis Sci 2012; 53:543-50. [PMID: 22199240].

84. Mutti D, Zadnik K, Fusaro RE, Friedman NE, Sboltz RI, Adams AJ. Lens in Childhood. Invest Ophthalmol Vis Sci 1997; 39:120-3. [PMID: 9430553].

85. Cheng T, Deng J, Xiong S, Yu S, Zhang B, Wang J, Gong W, Zhao H, Luan M, Zhu M, Zhu J, Zou H, Xu X, He X, Xu X. Crystalline Lens Power and Associated Factors in Highly Myopic Children and Adolescents Aged 4 to 19 Years. Am J Ophthalmol 2021; 223:169-77. .

86. Xiong S, He X, Sankaridurg P, Zhu J, Wang J, Zhang B, Zou H, Xu X. Accelerated loss of crystalline lens power initiating from emmetropia among young school children: a 2-year longitudinal study. Acta Ophthalmol 2022; 100:e968-76. .

87. He JC. A Theoretical Study on the Effect of Anterior Components of the Eye on Peripheral Refraction. Invest Ophthalmol Vis Sci 2010; 51:1724-.

88. He J. Thinning of Lens Thickness Might Be Responsible for Myopia Development. Invest Ophthalmol Vis Sci 2013; 54:1909-.

89. Fledelius HC. Myopia of prematurity, clinical patterns: A follow-up of Danish children now aged 3–9 years [Internet]. Vol. 73, Acta ophthalmologica Scandinavica. Hvidovre: Scriptor Publisher; 1995. p. 402–6.

90. Cook A, White S, Batterbury M, Clark D. Ocular growth and refractive error development in premature infants without retinopathy of prematurity. Invest Ophthalmol Vis Sci 2003; 44:953-60. [PMID: 12601014].

91. Lee YS, Chang SHL, Wu SC, See LC, Chang SH, Yang ML, Wu WC. The inner retinal structures of the eyes of children with a history of retinopathy of prematurity. Eye (Lond) 2018; 32:104-112. .

92. Moon S, Lee S, Caesar JA, Pruchenko S, Leask A, Knowles JA, Sinon J, Chaqour B. A CTGF-YAP Regulatory Pathway Is Essential for Angiogenesis and Barriergenesis in the Retina. iScience. 2020;23:1-35.

93. Chintala H, Liu H, Parmar R, Kamalska M, Kim YJ, Lovett D, Grant MB, Chaqour B. Connective tissue growth factor regulates retinal neovascularization through p53 protein-dependent transactivation of the matrix metalloproteinase (MMP)-2 gene. J Biol Chem 2012; 287:40570-85. .

94. Chen Z, Zhang N, Chu HY, Yu Y, Zhang ZK, Zhang G, Zhang BT. Connective Tissue Growth Factor: From Molecular Understandings to Drug Discovery. Front Cell Dev Biol 2020; 8:1-17. .

95. Yan L, Chaqour B. Cysteine-rich protein 61 (CCN1) and connective tissue growth factor (CCN2) at the crosshairs of

ocular neovascular and fibrovascular disease therapy. J Cell Commun Signal 2013; 7:253-63. [PMID: 23740088].

96. He L, Frost MR, Siegwart JT Jr, Norton TT. Altered gene expression in tree shrew retina and retinal pigment epithelium produced by short periods of minus-lens wear. Exp Eye Res 2018; 168:77-88. [PMID: 29329973].

97. Kumar V, Couser NL, Pandya A. Oculodentodigital Dysplasia: A Case Report and Major Review of the Eye and Ocular Adnexa Features of 295 Reported Cases. Case Rep Ophthalmol Med 2020; 2020:1-16. [PMID: 32318302].

98. Park DY, Cho SY, Jin DK, Kee C. Clinical Characteristics of Autosomal Dominant GJA1 Missense Mutation Linked to Oculodentodigital Dysplasia in a Korean Family. J Glaucoma 2019; 28:357-62. [PMID: 30628995].

99. Valiunas V, Polosina YY, Miller H, Potapova IA, Valiuniene L, Doronin S, Mathias RT, Robinson RB, Rosen MR, Cohen IS, Brink PR. Connexin. Connexin-specific cell-to-cell transfer of short interfering RNA by gap junctions. J Physiol 2005; 568:459-68. .

100. Szarka G, Balogh M, Tengölics Á, Ganczer A, Völgyi B, Kovács-Öller T. The role of gap junctions in cell death and neuromodulation in the retina. Neural Regen Res 2021; 16:1911-20. [PMID: 33642359].

101. Fischer AJ, McGuire JJ, Schaeffel F, Stell WK. Light-and focus-dependent expression of the transcription factor ZENK in the chick retina. Nat Neurosci 1999; 2:706-12. [PMID: 10412059].

102. Bitzer M, Feldkaemper M, Schaeffel F. Visually induced changes in components of the retinoic acid system in fundal layers of the chick. Exp Eye Res 2000; 70:97-106. [PMID: 10644425].

103. Pardue MT, Faulkner AE, Fernandes A, Yin H, Schaeffel F, Williams RW, Pozdeyev N, Iuvone PM. High susceptibility to experimental myopia in a mouse model with a retinal on pathway defect. Invest Ophthalmol Vis Sci 2008; 49:706-12. .

104. Schippert R, Burkhardt E, Feldkaemper M, Schaeffel F. Relative axial myopia in Egr-1 (ZENK) knockout mice. Invest Ophthalmol Vis Sci 2007; 48:11-7. [PMID: 17197510].

Articles are provided courtesy of Emory University and the Zhongshan Ophthalmic Center, Sun Yat-sen University, P.R. China. The print version of this article was created on 14 May 2023. This reflects all typographical corrections and errata to the article through that date. Details of any changes may be found in the online version of the article.